Heliyon 9 (2023) e22936

Contents lists available at ScienceDirect

Heliyon

journal homepage: www.cell.com/heliyon

Gut-immunity modulation in *Lepidocephalichthys guntea* during *Aeromonas hydrophila*-infection and recovery assessed with transcriptome data

Chandana Basak, Ranadhir Chakraborty *

OMICS Laboratory, Department of Biotechnology, University of North Bengal, Siliguri-734013, West Bengal, India

ARTICLE INFO

Keywords:
L. guntea
A. hydrophila
gut immunity
Heat shock response

ABSTRACT

The fish immune system, which consists of innate and adaptive immunologic processes, defends against viruses, bacteria, fungi, and parasites. The gut immunity is an integral part of the host immune system that controls immunological homeostasis, hosts' interactions with their microbiomes, and provides defence against a number of intestinal infections. *Lepidocephalichthys guntea*, a facultative air-breathing fish, was experimentally infected with *Aeromonas hydrophila* using intraperitoneal injection followed by bath challenge, and transcriptome data were used to examine the gut immune responses during disease progression and recovery from the diseased state without the use of medication. For the control or uninfected fish (FGC) and the infected fish that were kept for seven days (FGE1) and fifteen days (FGE2), separate water tanks were set up. Coding DNA sequences (CDS) for FGC and FGE1, FGC and FGE2, and FGE1 and FGE2 were analyzed for differential gene expression (DGE). The presence and expression of genes involved in the T cell receptor (TCR) signalling pathway, natural killer (NK) cell-mediated cytotoxicity pathway, and complement-mediated pathway, along with a large number of other immune-related proteins, and heat shock protein (HSPs) under various experimental conditions and its relationship to immune modulation of the fish gut was the primary focus of this study. Significant up-and-down regulation of these pathways shows that, in FGE1, the fish's innate immune system was engaged, whereas in FGE2, the majority of innate immune mechanisms were repressed, and adaptive immunity was activated. Expression of genes related to the immune system and heat-shock proteins was induced during this host's immunological response, and this information was then used to build a thorough network relating to immunity and the heat-shock response. This is the first study to examine the relationship between pathogenic bacterial infection, disease reversal, and modification of innate and adaptive immunity as well as heat shock response.

1. Introduction

Fish serves as a link between innate immunity and the formation of adaptive immunity since they are among the most numerous and diversified species of vertebrates to have evolved throughout the Devonian period. Despite certain differences, fish have an immune system that is biologically similar to higher vertebrates, such as humans. Fish immunity, however, is mostly attributed to their innate immune systems, which enable them to adapt to adverse environmental conditions [1,2]. In addition to the primary

* Corresponding author.
E-mail address: rcnbusiliguri@gmail.com (R. Chakraborty).

https://doi.org/10.1016/j.heliyon.2023.e22936
Received 24 May 2023; Received in revised form 20 November 2023; Accepted 22 November 2023
Available online 29 November 2023
2405-8440/© 2023 Published by Elsevier Ltd. This is an open access article under the CC BY-NC-ND license (http://creativecommons.org/licenses/by-nc-nd/4.0/).

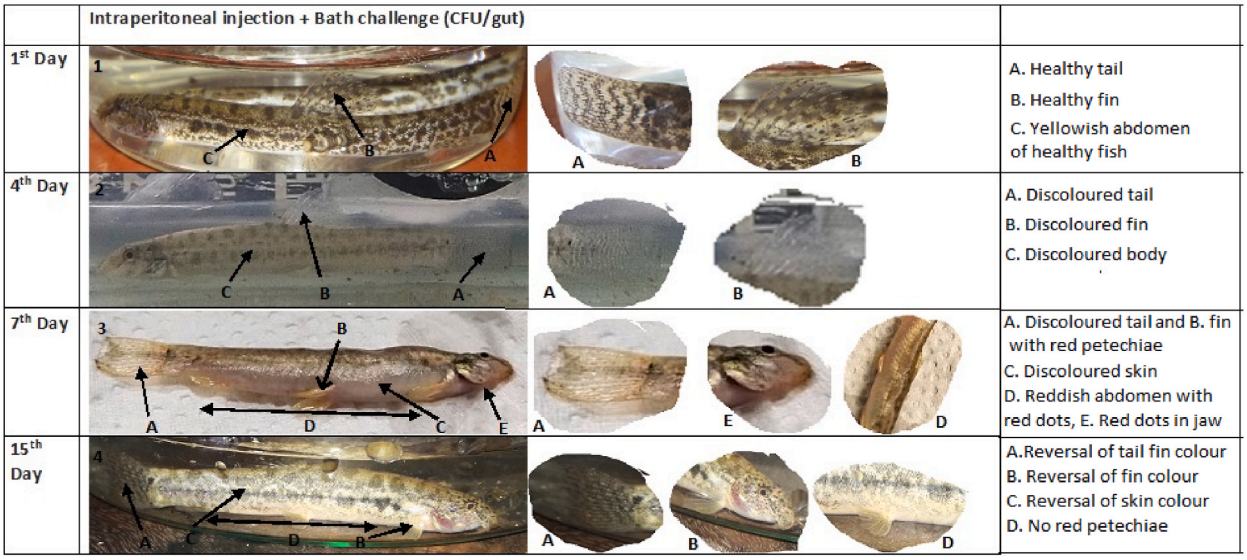

Fig. 1. The detailed illustration of the *L. guntea* disease model, include the onset of infection, the development of symptoms, and the resolution of the illness condition.

hematopoietic organ, fish have extra lymphoid tissues in several organs. Although fish lack the characteristic lymphocyte aggregation place known as Peyer's patches in mammals, the gut does contain a small number of leukocytes and macrophage-like cells [3]. In fish, innate immunity plays a critical role in preserving homeostasis through retaining a system of receptor proteins that recognise pathogen-associated molecular patterns (PAMPs), such as lipopolysaccharides, peptidoglycans, DNA, and RNA [4]. Warm-blooded vertebrates' immune systems and physiologies differ from those of fish, yet both are greatly influenced by the environment. Both innate and adaptive immune systems are influenced by environmental variables such as photoperiodism, temperature, and water oxygen content, which affect complement and lysozyme activity in the case of innate immunity and IgM concentration in the case of adaptive immunity [5]. In addition to environmental factors, certain variances are genetically transmitted and have evolved due to genetic changes. In the majority of cases, it manifests in the adaptive immune system, particularly in the form of genetic recombination, which is essential for the diversification of repertoires of lymphocyte-based antigen recognition receptors. Numerous aspects of fish immunity, including expression of immune-responsive genes, the process of inflammation and wound healing, antigen pattern recognition receptors, signalling, and lymphocyte trafficking, have not changed despite the diversification of the vertebrate phylum [6].

A widely studied intestinal pathogen called *Aeromonas hydrophila* is known to cause a number of diseases, including gastroenteritis, necrotizing fasciitis, and motile *Aeromonas* septicaemia [7,8]. *A. hydrophila* mostly functions as a secondary pathogen or opportunistic invader, and it can cause mass mortality if left untreated [9]. It can thrive in a wide temperature range from 0 to 45 °C (with an optimal range of 22–32 °C). Stresses like poor water quality, fish overcrowding, ineffective handling, and inefficient transportation are major predisposing factors establishing *Aeromonas* infections in aquaculture systems [10]. Fish infected with *Aeromonas* exhibit exophthalmia, ulceration with bright red spots, pale gills, irregular swimming, tail/fin rot, loss of appetite, and other signs [11]. The majority of farmed and wild freshwater fish, such as rainbow trout [12], carp [13,14], channel catfish [15], eels [16,17], zebrafish [18], goldfish [19], perch fish [20], tilapia [21], snakehead murrel [22], loach [23], and many more, are susceptible to *A. hydrophila* infection. Although studies on *Aeromonas* infection in loaches focused on the kidney, liver, spleen, muscles, and gut [23,24], they were typically limited to a bacteriological survey [25,26]. In particular, transcriptomics has opened up a new line of inquiry into the knowledge of immune-related proteins and how changes in infectious states affect their differential gene expression. As time goes on, these investigations have evolved to various omics levels. Although investigations on the intestinal responses to *Aeromonas* infection have not yet been published, studies on skeletal muscle [27], gill and liver [28], skin [29], gonads [30], intestinal air-breathing function and nutrition uptake and gas exchange [31,32], have been investigated in loach fish. Despite the fact that the gut-associated lymphoid tissues (GALTs) should have played a significant role in disease resistance among the four fundamental physical barriers created by a fish (gill-associated lymphoid tissues, skin-associated lymphoid tissues, mucosa-associated lymphoid tissues, and gut-associated lymphoid tissues), no research has been done to examine the pattern of immune response in the gut of loach fish under any pathogen-stress.

Lepidocephalichthys guntea, a cobitidae loach found in the Ganges and Brahmaputra river systems of northern India, Nepal, and Bangladesh, was selected for exploring the gut immune responses to *A. hydrophila* infection. This fish is able to live in eutrophic and slow-moving aquatic settings because of its capacity to breathe through the intestine [21]. The findings of this study open up a new field of study on fish gut immunity from the standpoint of the immunological response created by the gut cells when fish are exposed to *A. hydrophila*.

Table 1
Estimation of *A. hydrophila* population[a#] in the gut of *L. guntea* under different experimental conditions at different time periods.

	Bath challenge (CFU/mg wet weight of gut)	Intraperitoneal injection (CFU/mg wet weight of gut)	Intraperitoneal injection + Bath challenge (CFU/mg wet weight of gut)
1st Day (Before infection)	0.2 (± 0.04)	0	0
4th Day	27(± 1.63)	3.58×10^2(± 5.88)	8.2×10^4 (± 14.14)
7th Day	62(± 0.82)	1.82×10^2(± 1.63)	9×10^5 (± 12.25)
15th Day	–	–	18(± 0.82)

CFU/mg and $\geq 10^4$.
CFU/mg have been considered as the sub-clinical and clinical level respectively in accordance to the data (considered as clinical) obtained from the intestine of experimentally infected *Clarias batrachus* (5.6×10^4.
CFU/mg), *Labeo rohita* (7.7×10^5.
CFU/mg), *Cirrhinus cirrhosis* (5.8×10^5.
CFU/mg), and *Badis badis* (6.4×10^4.
CFU/mg) [20].
[a] , #, $\leq 10^2$.

Table 2
Distribution of coding DNA sequence in different gene ontology categories.

Sample Name	Biological Process	Cellular Component	Molecular Function
FGC	7528	7006	8082
FGE1	6476	6081	6876
FGE2	7420	6921	7935

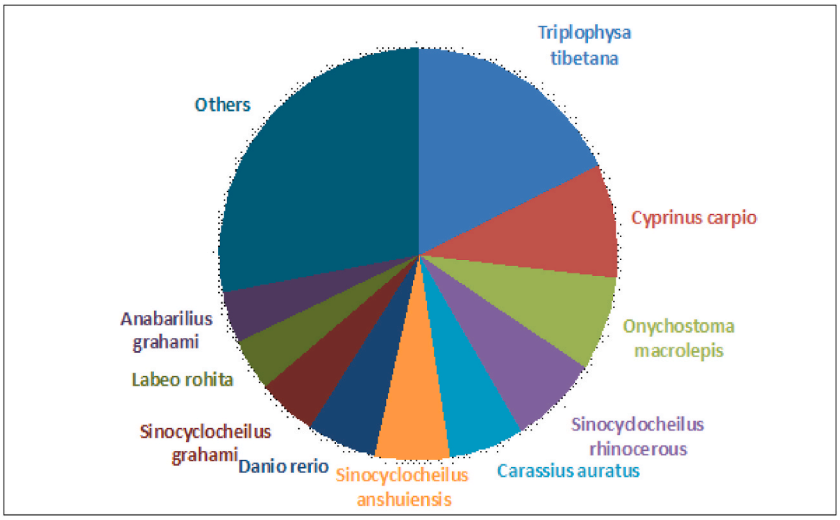

Fig. 2. Top 10 blast hit species distribution of pooled coding DNA sequence (CDS).

2. Result

2.1. Progression of A. hydrophila infection in the gut of L. guntea

No fish died and none showed any signs of disease even after being bath-challenged with *A. hydrophila* for seven days. In another experiment, fish were injected intraperitoneally with *A. hydrophila*, yet the fish displayed no disease symptoms. Fish that had been injected and subsequently subjected to the *A. hydrophila* bath challenge began exhibiting indications of the illness on day four, including skin discolouration, appetite loss, and inactivity. On day seven, symptoms reached their peak, with petechiae-like pinpoint red spots appearing in the fish's lateral region and the body becoming discoloured along with some grey dots in the head. There was no mortality noted throughout this trial, and after the 11th and 12th days, the health of the sick fish started to improve significantly. Fig. 1 depicts the progression of fish infection and disease recovery.

When challenges were applied individually, a culture-based investigation revealed that the load of *A. hydrophila* in fish guts on the fourth day of the 12 h bath challenge and the fourth day of the intraperitoneal injection was below the sub-clinical level ($\leq 10^2$ CFU/

Table 3
KEGG classification of coding DNA sequences (CDS) involved in several pathways related to the immune system of *L. guntea*'s gut.

Pathway Hierarchy	KEGG Pathway	CDS number		
		FGC	FGE1	FGE2
Immune system: [PATH:ko04062]	Chemokine signalling pathway	149	128	149
Immune system: [PATH:ko04621]	NOD-like receptor signalling pathway	143	128	147
Immune system: [PATH:ko04670]	Leukocyte *trans*-endothelial migration	124	101	117
Immune system: [PATH:ko04613]	Neutrophil extracellular trap formation	118	118	115
Immune system: [PATH:ko04611]	Platelet activation	112	119	119
Immune system: [PATH:ko04666]	Fc gamma R-mediated phagocytosis	104	82	98
Immune system: [PATH:ko04625]	C-type lectin receptor signalling pathway	102	87	107
Immune system: [PATH:ko04660]	T cell receptor signalling pathway	90	75	98
Immune system: [PATH:ko04620]	Toll-like receptor signalling pathway	84	77	98
Immune system: [PATH:ko04659]	Th17 cell differentiation	81	66	83
Immune system: [PATH:ko04650]	Natural killer cell mediated cytotoxicity	76	72	93
Immune system: [PATH:ko04662]	B cell receptor signalling pathway	75	57	77
Immune system: [PATH:ko04657]	IL-17 signalling pathway	70	69	74
Immune system: [PATH:ko04610]	Complement and coagulation cascades	66	70	64
Immune system: [PATH:ko04612]	Antigen processing and presentation	64	63	80
Immune system: [PATH:ko04664]	Fc epsilon RI signalling pathway	63	48	56
Immune system: [PATH:ko04622]	RIG-I-like receptor signalling pathway	61	56	65
Immune system: [PATH:ko04658]	Th1 and Th2 cell differentiation	58	41	61
Immune system: [PATH:ko04640]	Hematopoietic cell lineage	50	55	55
Immune system: [PATH:ko04624]	Toll and Imd signalling pathway	43	43	45
Immune system: [PATH:ko04623]	Cytosolic DNA-sensing pathway	36	32	36
Immune system: [PATH:ko04672]	Intestinal immune network for IgA production	26	25	23

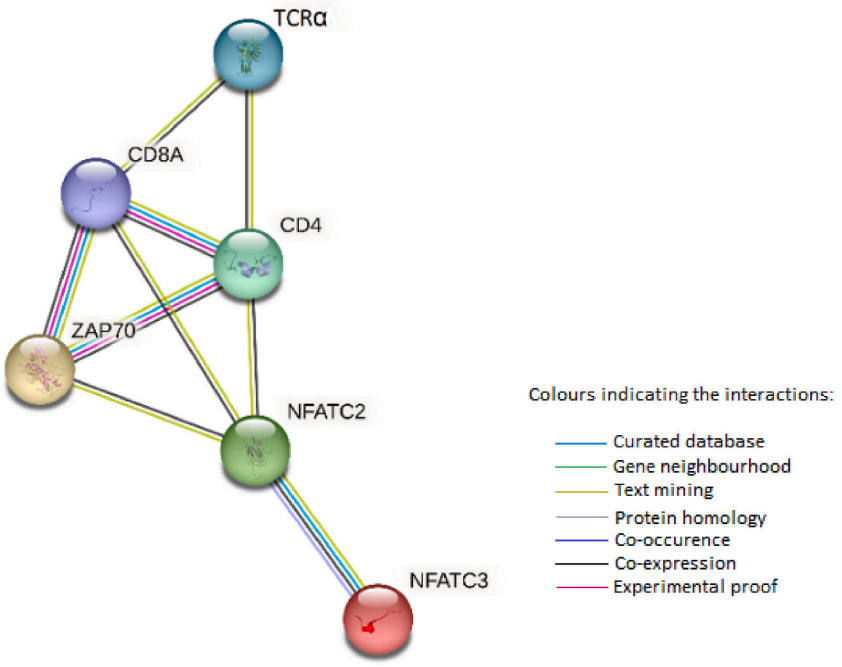

Fig. 3. Networking of T cell receptor signalling pathway working in gut of *L. guntea*.

mg). However, when both challenges were used at the same time, the mean pathogen load in *Aeromonas* selective agar was calculated to be 8.2×10^4 CFU/gut and 9×10^5 CFU/gut, on the fourth, and seventh days following infection, respectively (Table 1). This bacterial burden was once more below the sub-clinical range after 15 days. Therefore, bath challenge or intraperitoneal injection alone was insufficient for the creation of a disease model in *L. guntea*.

2.2. Sequencing and functional annotation

Whole transcriptome analyses of FGC, FGE1, and FGE2 produced 5.1 GB, 3.6 GB, and 6.7 GB high-quality paired reads respectively

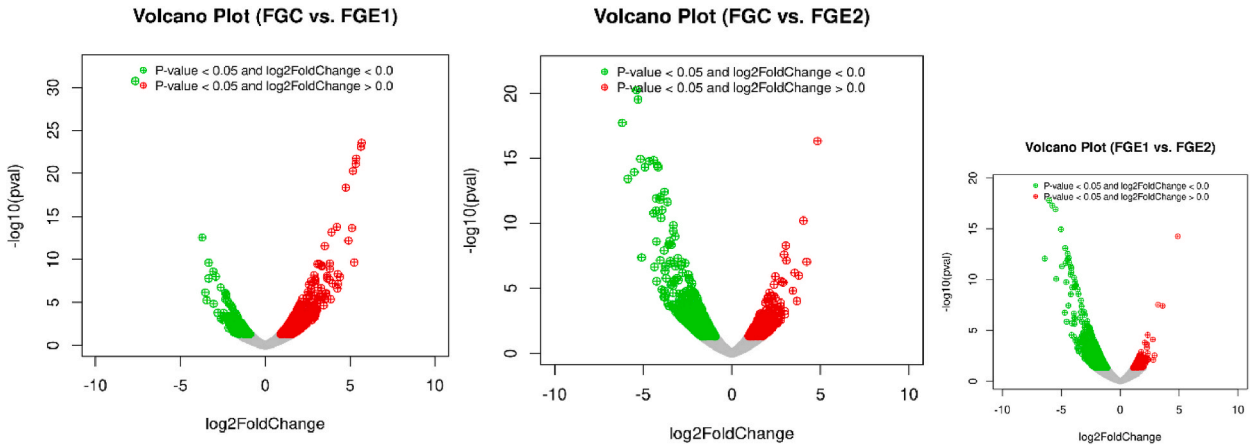

Fig. 4. Graphical representation of differentially expressed genes in three different combinations (Red blocks express significantly upregulated genes whereas green blocks represent significantly downregulated genes. Grey blocks show non-differentially expressed genes.).

that were pooled for de novo transcriptomics assembly. A total of 1, 49,847 transcripts (pooled) were assembled with a total transcript length (bases) of 125,026,132. In aggregate, 58,865 non-redundant validated unigenes were considered for further downstream analysis. A total of 31,331 CDS were pooled together, from which 27,437 CDS were functionally annotated. A sample-based CDS identification revealed that the FGC, FGE1, and FGE2 each comprised 20,868, 17,348, and 20,868 CDS, respectively. These gene product attributes were classified into three main domains: biological process (BP), molecular function (MF), and cellular components (CC) (Table 2), which were further subdivided into 48 categories using gene ontology (GO) analysis. The three samples' GO mapping revealed that the molecular function was connected with the highest number of CDS (Figs. S1, S2, and S3). The majority of the CDS were found to be homologous to *Triplophysa tibetana*, a stone loach, followed by *Cyprinus carpio*, a common carp, *Onychostoma macrolepis*, and a few other fish species, according to transcriptomic analysis (Fig. 2).

2.3. KEGG pathway analysis and detection of immune-responsive pathways

A total of 11,334, 10,127, and 11,660 CDS of FGC, FGE1, and FGE2 samples respectively were found to be categorized into 29 KEGG pathways under five main categories; metabolism, genetic information processing, environmental information processing, cellular process, and organismal systems. A total of 22 immune system-related pathways were found to be active in the gut of *L. guntea*, according to KEGG pathway analysis (Table 3).

FGC, FGE1, and FGE2 underwent a thorough KEGG pathway analysis to determine which immunological signalling pathways were active in each sample. The T cell receptor (TCR) signalling pathway functioning in FGC, FGE1, and FGE2 were compared to check the differences during different infectious conditions which revealed that TCR alpha chain (TCR-α), T-cell surface glycoprotein CD4, T-cell surface glycoprotein CD8 alpha chain (CD8A), tyrosine-protein kinase ZAP-70 and nuclear factor of activated T-cells cytoplasmic 2 (NFATC2) and nuclear factor of activated T-cells cytoplasmic 3 (NFATC3) are exclusively present in FGE2. Fig. 3 illustrates how various proteins associated with the adaptive immune system interact with one another in the fish gut. This interaction for all 6 proteins is demonstrated using co-expression and text mining. The three proteins CD8A, CD4, and ZAP70 are connected with one another via curated databases and experimental evidence, and NFATC2 and NFATC3 are correlating via curated databases and protein homology in addition to these two interactions. Interferon-gamma (IFN-ϒ) receptor 1 and granzyme B (GrB) are solely present in FGE1 and IFN-ϒ receptor 1, GrB, and Cluster of differentiation 48 (CD48) antigen present in FGE2, according to a pathway analysis of Natural killer (NK) cell-mediated cytotoxicity.

2.4. Differential gene expression (DGE) analysis

In combination 1 (FGC vs. FGE1), 651 genes were significantly upregulated and 197 genes were significantly downregulated. In combination 2 (FGC vs. FGE2), 392 genes were markedly upregulated and 583 genes were significantly downregulated, similar to combination 1. Combination 3 (FGE1 vs. FGE2) was made to compare the differences between the two experimental conditions, where 719 genes were significantly downregulated and 101 genes were significantly upregulated. Using volcano plots, Fig. 4 shows the distribution of DGEs.

2.5. Activation of complement system

A number of genes coding for complement components, including C1q3, C1q4, C4, C2, C2B, C3, C3a.1–1, C3-2, C7, C8α, C8b, three complement factors H, B, I, complement receptor type 2, complement C2-like isoform X1, mannose-binding protein (MBP), mannan-binding lectin serine protease 2 (MASP2), L-rhamnose-binding lectin (RBL), Intelectin, C-type lectin, and alpha-2-macroglobulin (A2M)

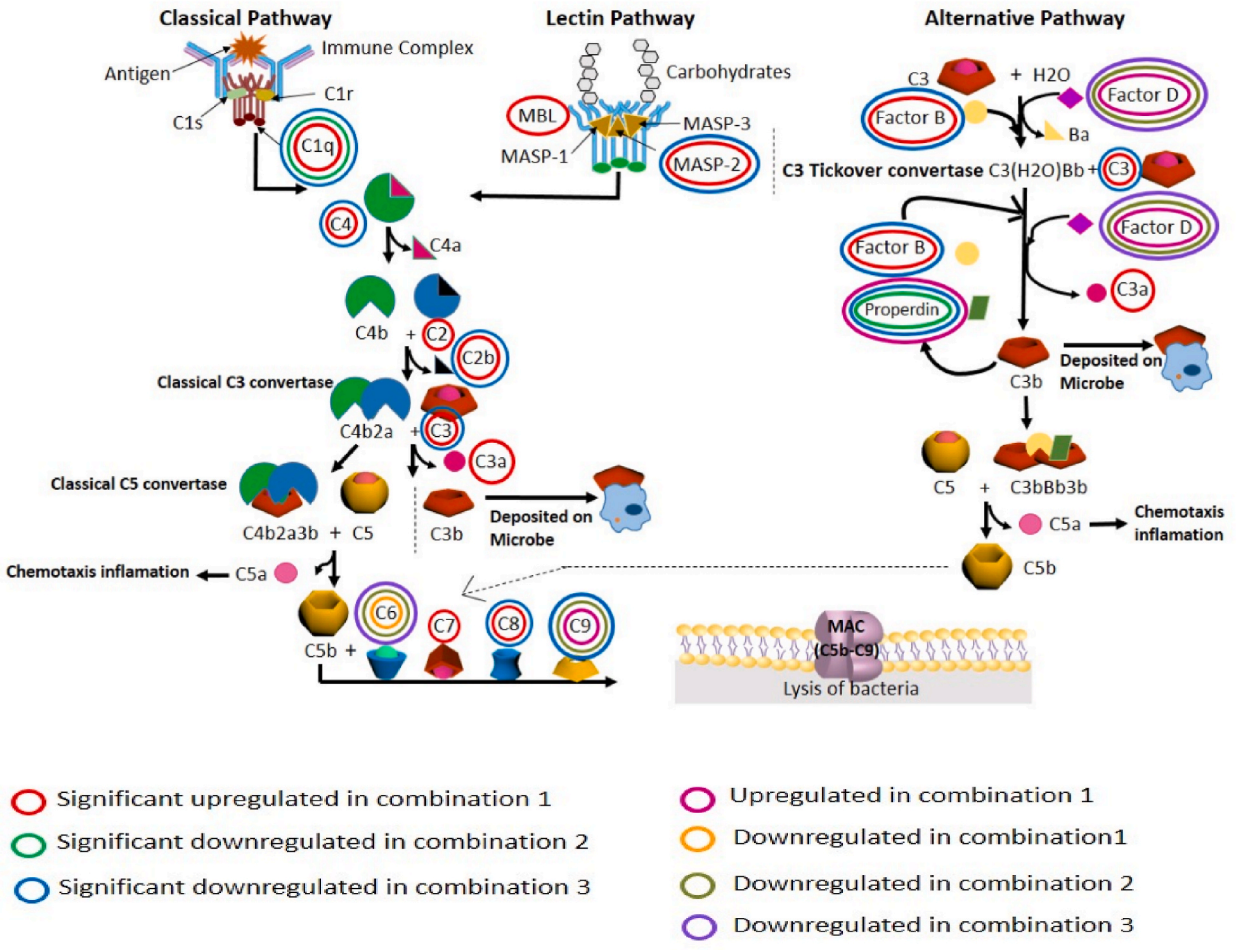

Fig. 5. Differential gene expression of complement components involved in three different complement mediated pathways working in the gut of *L. guntea*.

were significantly upregulated in combination 1 (Table S1) (Fig. 5). In combination 2, expression of genes coding for complement components C1q4, C1qa, and C-type lectin was considerably downregulated (Table S1). Further differential gene expression analysis was performed for combination 3 to assess whether there was a significant up-or-down-regulation of genes expressing complement pathway-related proteins in the two infection scenarios. Genes coding for several complement proteins, C1q3, C1q4, C1qa, C2B, C3, C4, C8α, C8b, C9, complement factors H, B, P or properdin, complement C2-like isoform X1, MBP, MASP2 and interlectin were significantly downregulated in FGE2 when compared to FGE1. Additionally, genes coding for complement factors D, P, and C9 were found to be upregulated in combination 1. Expression of genes coding for C6 and complement factor D were upregulated in combinations 2 and 3, while gene coding for C9 was downregulated in combination 2 (Fig. 5). Table S1 reflects a detailed description of FC values and the corresponding p values.

2.6. Differential expression of other immunity-related genes

A few other genes encoding immune response-related elements were found to be considerably expressed in both combinations. In combination 1, genes coding for interferon-induced Mx protein, meteorin, butyrophilin3, interferon regulatory factor (IRF), and interleukin-18 (IL-18) receptor were significantly expressed (Table S2). In combination 2, the significantly downregulated genes were those coding for vitellogenin, C type lectin, SLAM family member 9-like, NK cell receptor 2 B4-like isoform X2, lysozyme-like, cathepsin L, apolipoprotein A-I, follistatin-related protein 1 isoform X1, and intestinal mucin-like protein isoform X2. On the other hand, expressions of genes coding for interferon-inducible GTPase 5, IL-1 receptor, IFN-induced Mx protein, protein NLRC3, NACHT, LRR and PYD domains-containing protein 3 (NLRP3), and coronin-2A were significantly upregulated in combination 2 (Table S2).

In combination 1, differential gene expression analysis revealed a considerable up-regulation of genes coding for MHC class I antigen and the F10 alpha chain B–F histocompatibility in FGE1. With this, genes encoding H-2 class II histocompatibility antigen/I-E beta chain and I-related MHC class protein were found to be significantly down-regulated in combination 1 (Table S3). Genes coding

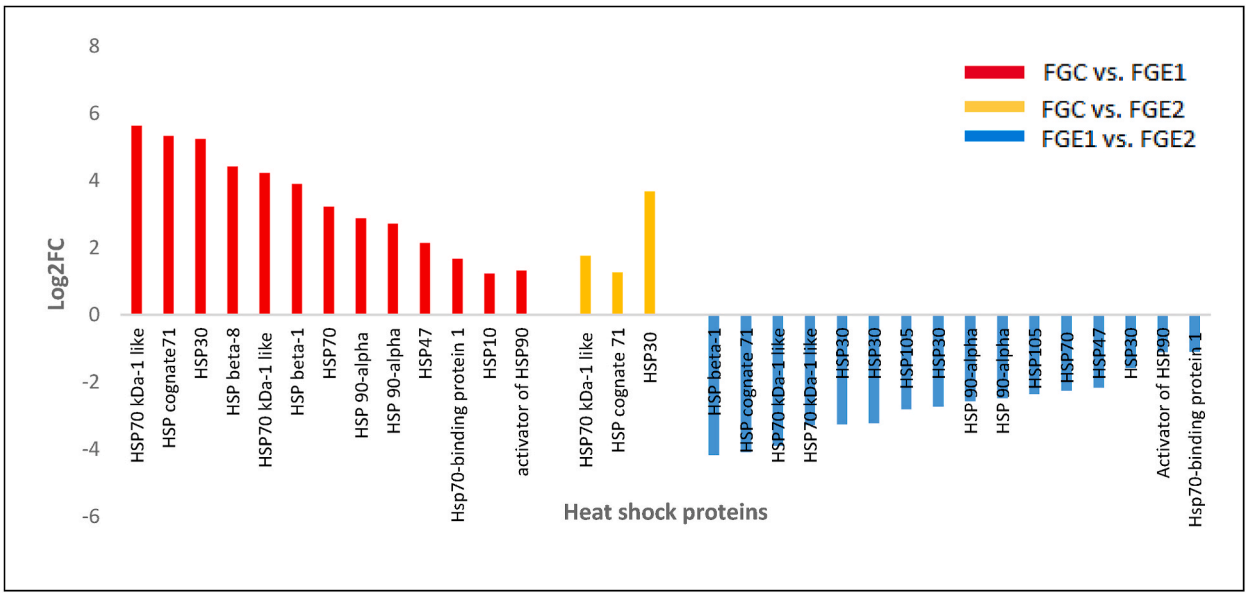

Fig. 6. Differential gene expression of heat shock proteins in the gut of *L. guntea* under three different experimental combinations. The fold change (FC) values were converted to Log2FC value for better representation. Red colour indicates the differential gene expression of FGC vs. FGE1 while yellow colour is the representative of FGC vs. FGE2 and blue colour represents FGE1 vs. FGE2.

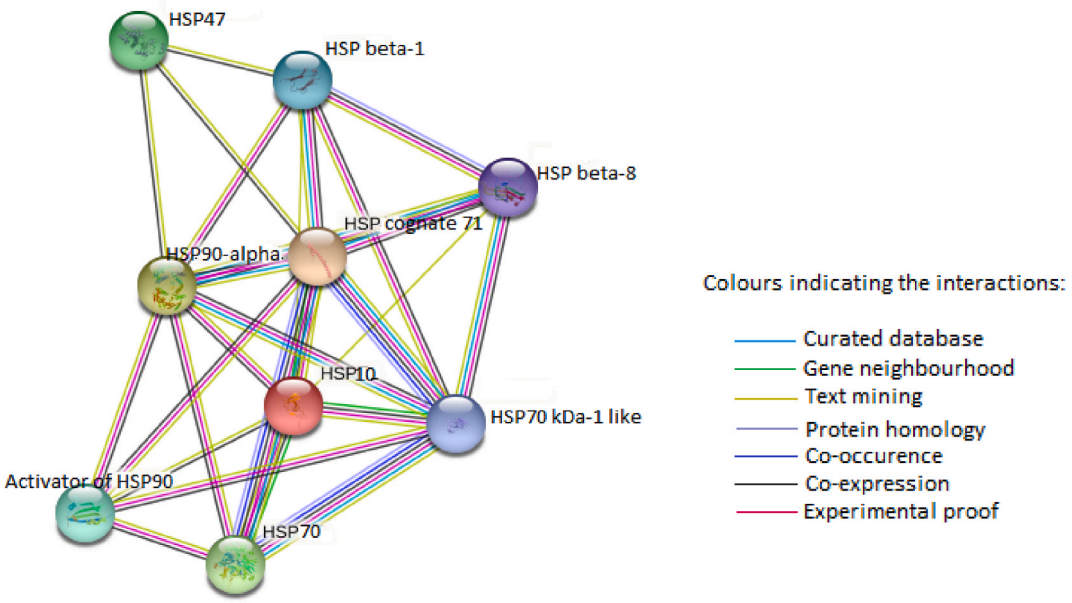

Fig. 7. Networking of significantly upregulated heat shock proteins of combination 1.

for F10 alpha chain B–F histocompatibility and MHC class I antigen were significantly upregulated in FGE2 compared to FGC (Table S3). Genes encoding transgelin-2 and various immunoglobulin (Ig) light chain 1, class II histocompatibility antigen, I-related proteins belonging to MHC class, and MHC class I antigen were also significantly downregulated in FGE2 as compared to FGC (Table S3).

2.7. Identification of heat shock proteins and their differential gene expression

In the transcriptome of *L. guntea*, expressions/transcripts of 23 HSP coding genes annotated, including Hsp 105, Hsp90α, Hsp90β, HSP90-1, Hsp 82, Hsp70, Hsp60, Hsp 47, Hsp 30, Hsp 18.1, Hsp-12.2, Hsp beta-11, Hsp10, Hsp beta-8, HSP beta-1, small heat shock

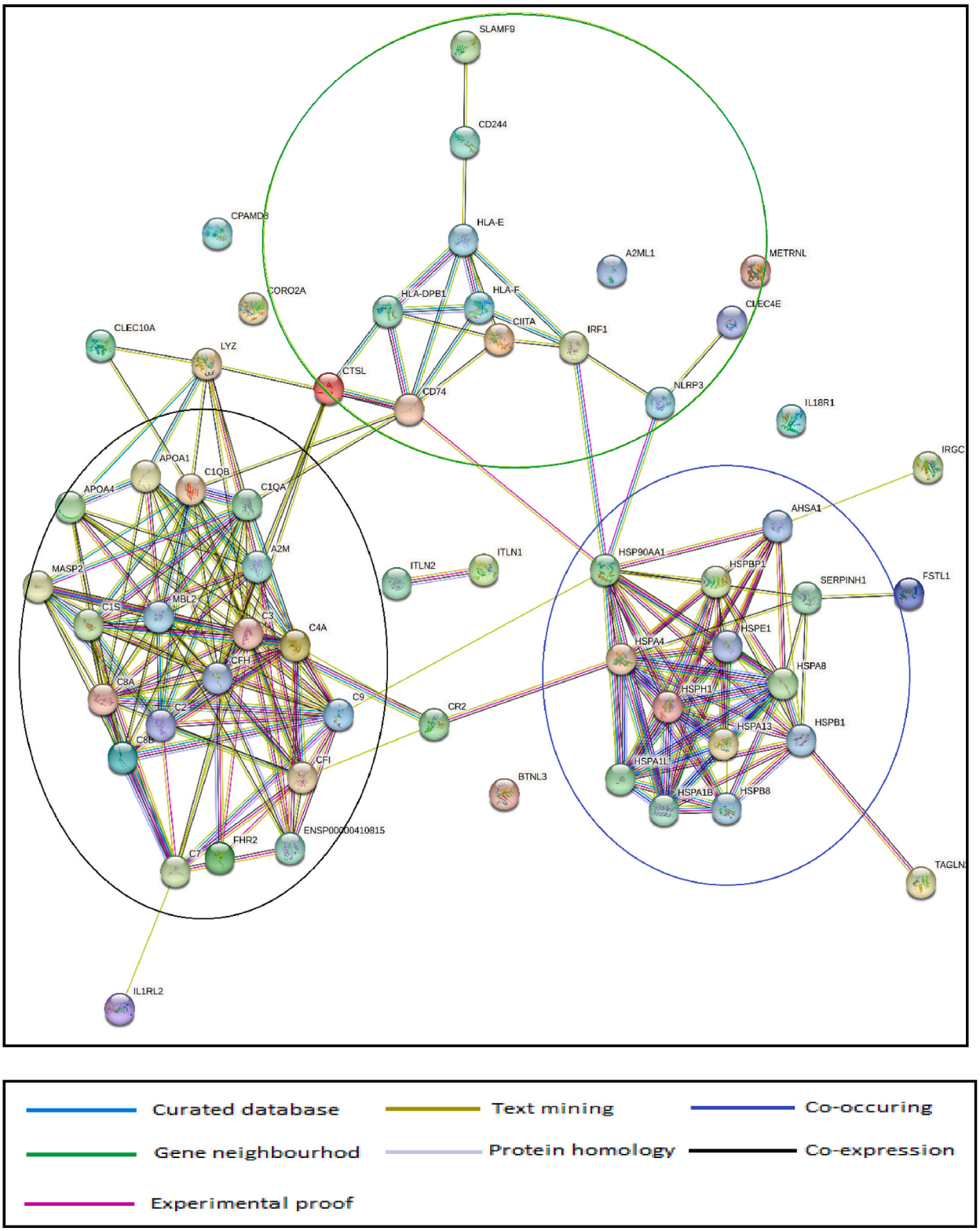

Fig. 8. Protein protein interaction network based on differentially expressed genes identified in *L. guntea*'s gut and mapped against the reference database of *Homo sapiens* in STRING v 11.0.

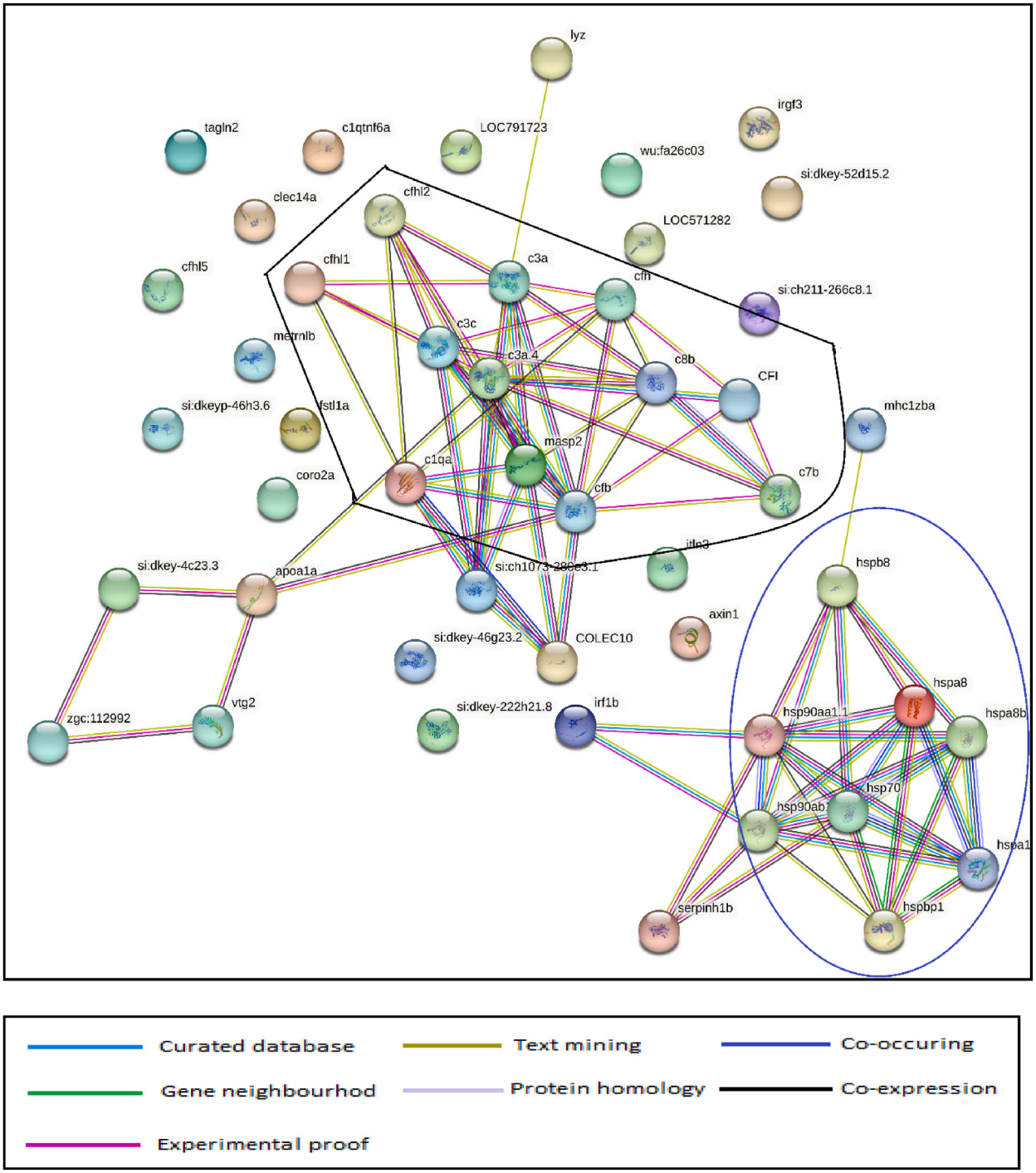

Fig. 9. Protein protein interaction network based on differentially expressed genes identified in *L. guntea*'s gut and mapped against the reference database of *Danio rerio* in STRING v 11.0.

protein OV25-1and two Hsp cognate71, Hsp cognate 40, HSP cognate 5, Hsp cognate4. Furthermore, genes coding for HSP5, HSP2, and HSP1 were also present.

The HSP genes with significantly greater expression levels in combination 1 were HSP70, HSP cognate71 (HSC71), HSP30, HSP70 kDa-1 like, HSP beta-8, HSP beta-1, HSP90-alpha, HSP-10, HSP47, and activator of HSP90 (Fig. 6). However, in FGE2, there was reduced expression of HSP genes except the ones coding for HSP70, HSP30, and HSP71 showing substantial up- or down-regulation (Fig. 6). Analysis of combination 3 has shown that the genes coding for HSP70 kDa-1 like protein, HSP70, HSP70 binding protein-1,

HSC71, HSP30, HSP beta-1, HSP105, HSP90-alpha, HSP47, and activator of HSP90 ATPase-like protein were significantly down-regulated in FGE2 as compared to FGE1. There was not much of an up-regulation of any genes expressing HSP proteins in this combination (Fig. 6). Table S4 lists the fold change values and corresponding p values.

Fig. 7 demonstrates that all proteins likely to be expressed via differential expression of HSP-coding genes, in combination 1, are connected to one another, at the very least through text mining and co-expression. While genes expressing Hsp10 and Hsp beta-8 activators of Hsp90 and Hsp70 were being related only by text mining, connections between Hsp beta-1 and Hsp beta-8 were made via protein homology and experimental evidence. Again, experimental proof links the activator of Hsp90 and Hsp cognate71 (HSC71) to Hsp beta-1 and Hsp90-alpha, Hsp90-alpha and activator of Hsp90, Hsp90-alpha and Hsp70, Hsp90-alpha and Hsp10, activator of Hsp90 and Hsp70, and activator of Hsp90 and Hsp70 like protein. Hsp beta-1 and HSC71, Hsp beta-8 and Hsp70 like, Hsp90 alpha and Hsp70 like are further linked with curated database and experimental proof. Furthermore, Hsp beta-8 and HSC71, HSC71 and Hsp90 alpha are linked via gene neighbourhood, experimental proof and curated database. Hsp70 and HSC71, HSC71 and Hsp70-like proteins are further interlinked via curated database, protein homology, co-occurrence and experimental proof. Hsp70 and HSC71 are linked via all seven types of interactions.

2.8. Comparative networking of proteins related to immunity and heat shock response

In order to create a protein-protein interaction network in the *L. guntea* gut following *A. hydrophila* infection, selected DEGs implicated in intestinal immune response and heat shock response were submitted to the STRING database and then mapped against the proteins database of Homo sapiens. This displayed high-order interactions between 54 nodes and 189 network edges (Fig. 8; p-value 1.0e-16). A number of proteins, including SLAM family member 9, NK cell receptor 2B4, MHC class I antigen, class II histocompatibility antigen, H-2 class II histocompatibility antigen, IRF1, cathepsin L1, NLRP3, C type lectin, lysozyme C, apolipoprotein A1 are interconnected via at least one interaction and up to five interactions (indicated by a green circle in Fig. 8). These are further connected to complement component and heat shock response related proteins (indicated by black circle and blue circle in Fig. 8). Again correlations between complement receptor type 2 with HSP70 and complement factor 9 with HSP90α highlight the fact that a fish's immune response to bacterial infection is linked to heat shock reaction as well (Fig. 8). The same DEGs were mapped against the proteins database of *Danio rerio* which showed a high-order interactions among 78 network edges and 47 nodes (Fig. 9; p-value <1.0e-16). A complement component pathway networking (indicated by a black circle in Fig. 9) along with vitellogenin and apolipoprotein was established and another on heat shock response (indicated by a blue circle in Fig. 9) was generated but both of them were not interlinked with each other (Fig. 9).

3. Discussion

The pathogenicity of *Aeromonas hydr*ophila is mediated by a range of surface polysaccharides, iron-binding systems, secretion systems, exotoxins, various extracellular enzymes, and adhesins, which primarily infect host cells as a secondary invader or opportunistic pathogen [33]. Failure of fish immunity poses a serious danger to commercial fish farming since diseases are expensive for an aquaculture system (cause mass death). Fish's intestinal immune system is constantly activated by antigens, immune modulators, and bacteria derived from the environment as a result of their feeding habit, which also makes the fish's digestive tract a key entrance point for unwanted pathogens [34]. The fish's gut-mucosal walls serve as immune systems and are directly involved in the prevention of disease by inducing a host immunological response. Gut-associated lymphoid tissue (GALT), which detects pathogens and interacts with the commensal mucosal microflora, is present in the epithelial layer and lamina propria of the intestine [35]. Although few studies on intestinal immune responses against *Aeromonas* spp. in grass carp [13], crucian carp [36], northern snakeheads [37], and Chinese sea bass [38] have been conducted, a thorough and practical knowledge of the immune system of fish, particularly that of loaches, is still lacking. In this study, transcriptome data on *Lepidocephalichthys guntea* is generated in an effort to better understand the mechanism of intestinal immune responses caused by *A. hydrophila* in loach.

We used a culture-based approach to detect the population of *A. hydrophila* in the gut of infected *L. guntea* followed by transcriptomics analysis of control (FGC) and experimental samples (FGE1, FGE2). A successful disease model was established when both intraperitoneal infection and bath challenge of *A. hydrophila* were used consecutively in the gut of *L. guntea*. A severe fish infection was noticed on the 7th day and disease reversal was observed on the 15th day of the initial infection (Table 1). Transcriptomics analysis showed that as compared to the FGC, FGE1 had a higher number of significant upregulated genes, while FGE2 had more significant down-regulating genes. According to prior research on grass carp [13], *A. hydr*ophila infection resulted in more up-regulated genes being detected in the intestine. The host's defence against infection was thus activated on the seventh day in *L. guntea*'s gut, and it gradually decreased over time, as detected on the 15th day post-experimental infection.

3.1. Innate immune response

Analysis of all of the complement components revealed that three independent complement pathways are working inside the gut of *L. guntea*. Combination 1 yielded significant up-regulation of several complement elements, including C1, C2, C3, C4, C7, and C8, complement factors H, B, and I, as well as complement receptors. According to a study on Chinese sea bass, the intestine of fish infected with *A. hydrophila* displayed a high up-regulation of complement components C4, C6, and C7, which ensured activation of complement-mediated classical pathways [13]. Similar results were observed in the intestine of gill head sea bream (*Sparus aurata* L.) after being exposed to a parasite (*Enteromyxum leei*) [39], and also in skin tissues of rainbow trout infected with Ich parasites [40]. Our

study shows that complement-mediated innate immunity was triggered and processed in the fish gut during the early stages of infection since FGE1 dramatically raised various elements of the lectin pathway, alternative pathway, and classical route (Fig. 5). The levels of all lectins that have previously been demonstrated to be involved in the innate immune response of grass carp [13] were markedly upregulated in FGE1 also. The majority of them work as pattern-recognition receptors (PRR), whose main function is to interact with bacterial carbohydrates and destroy the target by activating complement-mediated pathways [41]. Moreover, A2M, which is regarded as a complement component, was markedly elevated in combination 1 [42]. However, the first complement component's subcomponents C1q4 and C1qa were markedly downregulated in combination 2 (Fig. 5). Furthermore, combination 3 revealed that numerous complement components were significantly downregulated in FGE2 as compared to FGE1 (Fig. 5). The two comparisons provide evidence that complement-mediated immunity, which is part of innate immunity, quickly activates at the beginning of an infection, but gradually deactivates afterwards. In combination 2, NK cell receptor which is a part of innate immune system was downregulated (Table S2). Vitellogenin, C-type lectin and lysozyme all work as an innate immune component of host by acting as a multivalent pattern recognition receptor (PRR) followed by killing of bacteria [43–45] that were downregulated in combination 2.

SLAM family receptors and NK cell receptors are *trans*-membrane receptors expressed in immune cells and act as an innate immune component that provides first line of defence to the host [46]. Cathepsin L is also a part of innate immunity that helps in antigen processing and apolipoprotein A-I is known to reduce inflammation and their downregulation in FGE2 correlates with our hypothesis. Follistatin-related protein is again an innate immune component that can be activated by toll-like receptor 4 by interacting with CD14 [47]. Intestinal mucin-like protein acts as first line of defence, provides a layer of intestinal barrier and works as innate immune system. Expression of all these innate immunity-related genes was significantly downregulated in FGE2 (Table S2). In contrast, genes expressing NLRC3 family proteins were upregulated in FGE2, which control innate immunity and release pro-inflammatory cytokines [48] during inflammation and viral infection. NLRP3 plays a significant role in innate immunity by identifying microbial patterns and producing cytokines like IL1B and IL18 [49]. The transcription factor coronin-2A, which is required for the TLRs response [50] to begin, was once more increased in FGE2 (Table S2).

3.2. Crosstalk between innate and adaptive immunity

Several other immune response-related elements like meteorin, butyrophilin3, interferon-induced Mx protein, IRF, and IL-18 receptor were found to be considerably elevated in combination 1 (Table S2). A particular class of cytokine called meteorin-like protein has recently been discovered in grass carp. This protein is released by activated macrophages when other cytokines and lipopolysaccharides trigger it [51]. Butyrophilin3 has been linked to adaptive immunity in fish and higher vertebrates, according to reports from Asian seabass and *Channa striatus* [52]. Although the function of Mx proteins during bacterial infection is poorly understood, interferon-induced Mx proteins are generally known to play a vital role in antiviral immunity [53]. The growth of dendritic cells as well as the differentiation of monocytes into macrophages depends on IRF. Additionally, dendritic cells serve as a link between innate and adaptive immunity [54]. The cell surface receptor for IL-18 is called the IL-18 receptor. IL-18 plays an essential role in mediation of inflammatory response after pathogen invasion and this pro-inflammatory cytokine can regulate both innate and adaptive immunity. After pathogen invasion, IL-18 plays a crucial role in mediating the inflammatory response, and this pro-inflammatory cytokine can control both innate and adaptive immunity [55]. The significant up-regulation of genes coding for MHC class I antigen, F10 alpha chain B–F histocompatibility complex (Table S3), and immune response-related components (Table S2), indicates that the interaction between innate and adaptive immunity in the fish gut began on the seventh day of infection. However, the down-regulation of H-2 class II histocompatibility antigen and I-related gene protein MHC class seen in combination 1 (Table S3) could not be explained since *L. guntea*'s defensive mechanism against *A. hydrophila* invasion is little understood.

3.3. Adaptive immune response

T cell lymphocytes and B cell lymphocytes make up fish's adaptive immunity. T cells create four different types of T lymphocytes, which give cellular immunity against pathogen invasion, and B cells produce immunoglobulin (Ig), which provides antibody-mediated protection [56]. As they convey the antigen to T cells, the major histocompatibility complex (MHC) plays a crucial function in the activation of T lymphocytes. Fish have a restricted expression of MHC class II compared to a widespread distribution of MHC class I [57]. Therefore up-regulation of F10 alpha chain B–F histocompatibility and MHC class I antigen confirms the activation of adaptive immunity, but at the same time marked down-regulation of immunoglobulin (Ig) light chain 1, class II histocompatibility antigen, I-related gene protein MHC class, and MHC class I antigen in combination 2 strangely contradicts our notion (Table S3). An actin-binding protein called transgelin-2 can help immunological synapse stabilization when T cells are unable to react to antigen-presenting cells (APC) [58]. Transgelin-2 down-regulation in combination 2 demonstrates that T cell activation occurs on day 15 of infection.

When Atlantic salmon was challenged with the bacterium, *Piscirickettsia salmonis,* to study infection on the head kidney, differential gene expression analysis supported the activation of innate immunity and the suppression of adaptive immunity [59,60]. The pathology of bacterial intracellular infection entails a constant battle between the host's immune system and the bacterium's unique defence systems. This host-specific process also known as cell-autonomous immunity includes cytokines, chemotactic migration of immune cells towards infection, avoiding lysosomal toxicity and autophagy. Interferon, which promotes gene expression in response to bacterial infection, mediates cell-autonomous immunity [61]. As per detection of immune responsive pathways using KEGG analysis, after infection, IFN- ϒ expresses quickly and is important for the innate immune response because it activates NK cells and

macrophages, which in turn triggers the adaptive immunological response [62]. GrB plays a role in both innate and adaptive immunity as it is released upon activation from NK cells and cytotoxic T cells [63]. However, CD48 antigen is a potential marker of B cell development and also plays a role in the activation of T cells, APCs, and granulocytes, its presence in FGE2 strongly suggests that adaptive immunity was activated at a later infection stage [64]. We discovered the presence of Von Willebrand factor solely in both experimental situations while analysing the platelet activation pathway. Kindlin 3 only appeared in FGE2. This protein is produced in hematopoietic cells and endothelial cells. It plays a crucial role in integrin modulation and is implicated in the activation of T cells and neutrophils [65]. In FGE2, the presence of many T cell-related proteins including ZAP-70 indicates that the fish gut's adaptive immune response has begun to function (Fig. 3). The T cell is activated by the TCR complex, which functions as an extracellular signal. The MHC and T-cell surface glycoprotein CD4 and CD8 are co-receptors on TCR that can identify antigens linked to them, stabilising the association with MHC [66]. The outcome of CD3 tyrosine phosphorylation, ZAP-70, stimulates TCR and relieves autoinhibited TCR, which in turn causes T cell clonal growth and lymphokine production [67] (Fig. 3). NFATC2 activates T cell gene transcription during an immune response, and NFATC3 controls T cell and immature thymocyte gene expression, so triggering the immune response's downstream cascades. They both go on to increase the production of various interleukins [68].

3.4. Heat shock response

Heat shock proteins are highly expressed in aquatic species in response to a variety of external stimuli, including temperature shock, chemicals, medications, pathogens, etc. [69]. In this study, considerable overexpression of HSP70 was observed in the gut of infected *L. guntea* in combination 1. HSP70 expression increased in combination 2 also, but it was less so than in combination 1 (Fig. 6). HSP70 can increase the production of a number of cytokines, which suggests that it is implicated in both innate and adaptive immunity [70]. The immunological signalling cascade was previously known to be prevented by HSC71 during viral infection, but its function during bacterial infection is unclear [71]. However, in both experimental settings, expression of HSC71 was markedly increased, suggesting that it may possibly be implicated in bacterial infection (Table S4). HSP90 and it's activator were found to be significantly upregulated in FGE1, but not in FGE2 (Fig. 6). As a molecular chaperone that controls intracellular transport, protein stabilization, protein degradation, and cell signalling. HSP90 is known to regulate a wide range of crucial cellular and molecular processes. In addition to this, HSP90 can operate as a ligand by interacting with numerous cell surface receptors, activating immunological responses similar to TOLL and differentiation clusters (CD14 or CD91) [72]. According to a transcriptome study on Mandarin fish infected with the bacterium, *Flavobacterium columnare*, HSP90 and HSP70 were found to be down-regulated during infection. This was thought to be the result of *F. columnare* using HSP homologues (HtpG and DnaK) to properly fold its own proteins [73]. Studies on shrimps challenged with the bacterium, *Vibrio*, and rainbow trout infected with single-celled ciliated protozoan, *Ichthyophthirius multifiliis*, have revealed highly upregulated HSPs that are known to affect innate immunity [74,75]. In our study, the abundance of bacteria in the fish gut causes a robust expression of various HSPs in combination 1 and a weaker expression as well as the absence of those HSPs in combination 1 (Table S4), indicating that most of the heat shock proteins, which are also connected to immune system function, are present in the early stages of infection. In the later stages of infection, expression of HSPs declines, which could be associated with fish health recovery. Fig. 7 demonstrates that, after being infected with *A. hydrophila*, a heat shock response has been generated in *L. guntea*'s gut as evident on the seventh day of the initial infection and all the heat shock response-related components work together in a comprehensive manner.

3.5. Networking of gut immunity and heat shock response

In order to create a protein-protein interaction network, DEGs of the intestinal immune system and the heat shock response in *L. guntea* following *A. hydrophila* infection was mapped to the protein databases of *Homo sapiens* and *Danio rerio*. A robust network of interactions was built with corresponding information available from that of *Homo sapiens*. This comparative networking is very helpful to close the knowledge gap in the field of fish immunology and pathway establishment of its related proteins because the majority of these proteins are related to innate immunity and fishes share a great homology with other vertebrate animals (including humans).

4. Conclusion

The elaborate immune system of *L. guntea* prevents the spread of intracellular infections and produces a potent immune response in the event of pathogen invasion. The host's physiological defences were breached in cases of intraperitoneally injected *A hydrophila* followed by a bath challenge. As a result, indications of a severe disease appeared seven days after the initial infection and disappeared on day fifteen. In the fish gut on the seventh day after infection, the innate immune system was very active, and there was also evidence of a cross-talk between the innate and adaptive immune systems. On the 15th day of infection, the majority of the genes coding for innate immunity-related proteins were down-regulated and the adaptive immune response was triggered. As a result, on the seventh day of infection, there was a large up-regulation of heat shock proteins, most of which disappeared after the fish's health had improved on the fifteenth day.

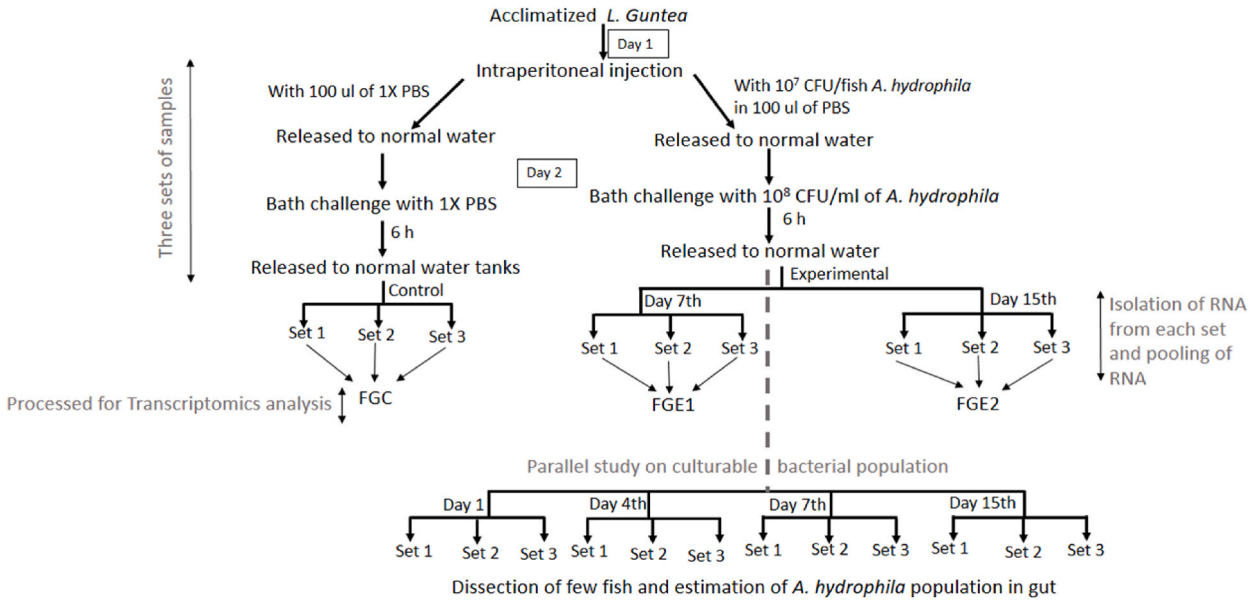

Fig. 10. Schematic representation of the experimental design established to study *A. hydrophila* infection and gut immunity in *L. guntea*.

5. Materials and method

5.1. Ethics statement

All experiments were conducted under the guidance of Committee for the purpose of control and supervision of experiments on animals (CPCSEA) for experimentation on fishes (http://cpcsea.nic.in/WriteReadData/LnPdf/GuidelinesofCPCSEAforExperimentationonFishes-2021.pdf) through Institutional Animal Ethics Committee (Approval No. IAEC/NBU/2022/32).

5.2. Experimental design and method of infecting guntea loach with A. hydrophila

5.2.1. Collection and maintenance of fish

Wild guntea loaches with varying lengths (7.3 cm–9.1 cm) and weights (5.6 g–7.5 g) were taken from North Bengal University's Magurmari River (26.710187° N, 88.357797° E) and transported to the lab in glass containers containing fresh river water. After that, the fish were moved to a 500 l tank with de-chlorinated water and aeration for 15 days so that they could get used to the laboratory environment and so that observations could be made, such as detecting any deformities or deaths (if any), could be made. The fish were fed once daily while maintaining standard water quality parameters such as dissolved oxygen (6.3–6.8 mg/l), pH (6.5–6.8), ammonia (0.3–0.5 mg/l), and temperature (24–26 °C).

5.2.2. Preparation of A. hydrophila for infection study

Aeromonas hydrophila MCC 2052^{T} was cultured in nutrient agar (HiMedia) at 30 °C using a pure culture that was obtained from the NCMR culture collection centre in Pune, India. Following the standard microbiological method, the fresh log-phase grown culture was centrifuged at 4000 RPM for 10 min and pellet was re-suspended in sterile PBS and added to the experimental tanks for bath challenge such that the density of *A. hydrophila* attained was 1×10^8 CFU/ml [22]. A dose of 1×10^7 CFU of *A. hydrophila* (in PBS) per fish was used as intraperitoneal injection [20].

5.2.3. Bath challenge and intraperitoneal injection with A. hydrophila both separately and combined

Healthy fish were subjected to bath challenges for 6, 8, 10, and 12 h in each of the four experimental tanks before being moved to four distinct normal water tanks without an *A. hydrophila* culture [76] (Fig. S4). In each bath challenge, the mortality (if any) was tracked for 7 days after infection. A batch of healthy fish was released into normal water in separate tanks after receiving intraperitoneal injections of a bacterial suspension (100 μl of PBS containing 1×10^7 CFU *A. hydrophila*) in a distinct disease model setup [24]. The fish were sacrificed at the first, fourth, and seventh days after the initial infection, and their guts were dissected, homogenized (with micro-pestle) in PBS, and serially diluted for plating in selective *Aeromonas* agar for determining the viable *A. hydrophila* count (Fig. S4).

In a separate experiment, after receiving an injection of *A. hydrophila* (1×10^7 CFU/fish) on day one, a group of fish were given a bath challenge (1×10^8 CFU/ml *A. hydrophila* rich water) for 6 h on next day before releasing them in normal water (Fig. S1). To

examine the effectiveness of infection and the establishment of disease infection in *L. guntea*, this experiment was carried out in triplicate.

5.3. Sample preparation for final experiment and RNA isolation

Water tanks were sterilised with potassium permanganate according to conventional procedures for the final experiment. These tanks were designated as the control (FGC), experimental 1 (FGE1), and experimental 2 (FGE2) tanks. Fifteen acclimated, healthy fish were housed in each tank, which was filled with 100 l of water and maintained according to all previously standardised quality measures (Fig. 10). To create the disease model, the other fish in two experimental tanks received bacterial injections on day 1 and were then challenged with *A. hydrophila* as described above. Control fish received 100 μl of 1X PBS as a control injection. For both the control and experimental groups, three replicates were put up concurrently. The emergence of symptoms resembled disease models developed in experiments. Fish from FGE1 (three replicates) and FGE2 (three replicates) were sacrificed on days 7 and 15, respectively. Fish guts were dissected and distributed into nine sets in total, comprising three replicates of each FGC, FGE1 and FGE2 being removed separately while preserving aseptic conditions. Using the traditional Trizol procedure with some slight changes, RNA was recovered from each of nine sets of dissected fish guts. Three replicates of the FGC's RNA samples were later combined. The same approach was used for FGE1 and FGE2. For the transcriptomics study, three sets of pooled RNA samples-FGC, FGE1 and FGE2-were used. On the other hand, a concurrent culture-based study was conducted on days 1, 4, 7, and 15 to estimate the population of *Aeromonas hydrophila* in fish guts (Fig. 10).

5.4. 5.4. RNA sequencing

The qualities and quantities of the isolated RNA samples were checked on 1 % denaturing RNA agarose gel and Nanodrop, respectively followed by Agilent Tape station using High Sensitivity RNA screen tape. The RNA-Seq paired-end sequencing libraries were prepared using the Illumina TruSeq Stranded mRNA Prep kit. Briefly, mRNA was enriched from the total RNA using Poly-T attached magnetic beads, followed by enzymatic fragmentation, 1st strand cDNA conversion using SuperScript ll and Act-D mix to facilitate RNA-dependent synthesis. The 1st strand cDNA was then synthesized to second strand using the second strand mix. The dscDNA was then purified using AMPure XP beads followed by A-tailing, adaptor ligation and then enriched by limited no. of PCR cycles. Quantity and quality check of the library was performed on Agilent 4200 tape station using high sensitivity D1000 Screen tape. After obtaining the Qubit concentration for the libraries and the mean peak sizes from the Agilent Tape Station profile, the PE Illumina libraries were loaded onto the Illumina Platform (HiSeq 2500) for cluster generation and sequencing. Paired-end sequencing allows the template fragments to be sequenced in both the forward and reverse directions on the Illumina platform.

5.5. Pre-processing of reads and de novo transcriptomic assembly

The sequenced raw data for the FGC, FGE1 and FGE2 samples were processed to obtain high-quality concordant reads using Trimmomatic v0.38 [77] and an in-house script to remove adapters, ambiguous reads (reads with unknown nucleotide "N" larger than 5 %), and low-quality sequences (reads with more than 10 % quality threshold (QV) < 20 phred scores). The high-quality (QV > 20), paired end reads were used for de novo assembly of the samples. The filtered high-quality reads of the FGC, FGE1 and FGE2 samples were pooled together and assembled into transcripts using Trinity de novo assembler (V2.5) with a k-mer of 25 and minimum contig length of 200 [78]. The assembled transcripts were then further clustered together using CD-HIT-EST-4.6 to remove the isoforms produced during assembly [79].

5.6. Quality control and functional annotation

This resulted in sequences that can no longer be extended and such sequences were defined as unigenes. Unigenes having >80 % coverage at 3X read depth were considered for downstream analysis. TransDecoder-v5.3.0 (http://transdecoder.github.io/) was used to check the chimeric rate during assembly and to predict coding sequences from the above-mentioned unigenes. Functional annotation of the genes was performed using the DIAMOND programme which is a BLAST-compatible local aligner for mapping translated DNA query sequences against a protein reference database [80]. DIAMOND finds the homologous sequences for the genes against NR (non-redundant protein database) from NCBI.

5.7. Sample-wise CDS identification, gene ontology and pathway analysis

For sample-wise coding DNA sequence (CDS) identification from above mentioned pooled sets of contigs, reads from FGC, FGE1 and FGE2 samples were mapped on the final set of pooled contigs using the BWA (-mem) toolkit. The read count (RC) values were calculated from the mapping results and those CDS having 80 % coverage and 3X read depth were considered for downstream analysis. To classify the functions of predicted contigs, gene ontology analysis (GO) for each of the samples, was carried out using the Blast2GO programme [81]. BlastX result accession IDs were used to retrieve gene names or symbols which were then searched in the species-specific entries of the gene product table of GO database. BlastX result accession IDs were used to retrieve UniProt IDs making use of PIR which include PSD, UniProt, SwissProt, TrEMBL, RefSeq, GenPept and PDB database. To identify the potential involvement of the predicted CDS in biological pathways, the CDS of FGC, FGE1 and FGE2 samples were mapped individually to reference canonical

Table 4
Combinations followed to evaluate differentially expressed genes (DEGs) in the gut of *L. guntea* in response to *Aeromonas hydrophila* infection.

Control	Vs.	Treated	Description
FGC	Vs.	FGE1	Combination 1
FGC	Vs.	FGE2	Combination 2
FGE1	Vs.	FGE2	Combination 3

pathways in KEGG. The output of KEGG analysis includes KEGG orthology (KO) assignments and corresponding enzyme commission (EC) numbers and metabolic pathways of predicted CDS using the KEGG automated annotation server, KAAS [82].

5.8. Differential expression analysis

Differential expression analysis was performed on the contigs between control and treated samples by employing a negative binomial distribution model in the DESeq package (version 1.22.1) [83]. Dispersion values were estimated with the following parameters: method = blind, sharing mode = fit only and fit type = local. P value adjustment was performed using a false discovery rate controlling procedure. Log2 fold change was calculated on the read abundance using the formula: FC = Log2 (Treated/Control). The CDS having a log2 fold change value greater than zero was considered as up-regulated whereas less than zero was downregulated. P-value threshold of 0.05 was used to filter statistically significant results. The contigs with an adjusted p-value <0.05 and a fold change larger than 2 were counted as significantly differentially expressed between the combinations followed for DGE (Table 4) [84]. For extensive studies of specific pathways, contigs with fold change larger than 2 and p-value <0.05 but not meeting the criteria of adjusted p-value were also considered [85].

5.9. Protein network analysis

The Search Tool for the Retrieval of Interacting Genes/Proteins (STRING; version 11.0) database [86] was used to perform protein network analysis of the TCR signalling pathway and heat shock pathway, with *Homo sapiens* (NCBI taxonomy id: 9606) as the reference. A detailed comparison of differentially expressed genes related to fish intestinal immunity and heat shock response was performed using the STRING database against two different reference organisms; *Homo sapiens* and *Danio rerio* (NCBI taxonomy id: 7955). Only the first shell of contact was allowed with a medium confidence interaction score cut-off of 0.400 [87]. The edges (protein-protein interaction) and nodes (initial shell of interaction) were coloured differently, with red, light blue, green, and yellow denoting interactions from gene fusions, curated databases, gene neighbourhood, and text mining, respectively. Similarly, pale blue, dark blue, black, and purple lines represent different sources of relationships such as protein homology, co-occurrence, co-expression, and experimental proof.

Funding information

This work was supported by the University of North Bengal [Sanc. No. 499/R2020 dt. 01-06-2020].

CRediT authorship contribution statement

Chandana Basak: Data curation, Formal analysis, Investigation, Writing – original draft. **Ranadhir Chakraborty:** Conceptualization, Data curation, Formal analysis, Funding acquisition, Investigation, Methodology, Supervision, Writing – original draft, Writing – review & editing.

Declaration of competing interest

The authors declare that they have no known competing financial interests or personal relationships that could have appeared to influence the work reported in this paper.

Acknowledgements

One of the authors, CB is thankful to the Council of Scientific and Industrial Research, India for a senior research fellowship.

Appendix A. Supplementary data

Supplementary data to this article can be found online at https://doi.org/10.1016/j.heliyon.2023.e22936.

References

[1] D.A. Plouffe, P.C. Hanington, J.G. Walsh, E.C. Wilson, M. Belosevic, Comparison of select innate immune mechanisms of fish and mammals, Xen 12 (2005) 266–277, https://doi.org/10.1111/j.1399-3089.2005.00227.x.

[2] L.Y. Zhu, L. Nie, G. Zhu, L.X. Xiang, J.Z. Shao, Advances in research of fish immune-relevant genes: a comparative overview of innate and adaptive immunity in teleosts, Dev. Comp. Immunol. 39 (2013) 39–62, https://doi.org/10.1016/j.dci.2012.04.001.

[3] J.H.W.M. Rombout, H.B.T. Huttenhuis, S. Picchietti, G. Scapigliati, Phylogeny and ontogeny of fish leucocytes, Fish Shellfish Immunol. 19 (2005) 441–455, https://doi.org/10.1016/j.fsi.2005.03.007.

[4] A. Rebl, T. Goldammer, Under control: the innate immunity of fish from the inhibitors' perspective, Fish Shellfish Immunol. 77 (2018) 328–349, https://doi.org/10.1016/j.fsi.2018.04.016.

[5] T.J. Bowden, Modulation of the immune system of fish by their environment, Fish Shellfish Immunol. 25 (2008) 373–383, https://doi.org/10.1016/j.fsi.2008.03.017.

[6] A. Castillo, C. Sanchez, J. Dominguez, S. Kaattari, A. Villena, Ontology of IgM and IgM-bearing cells in rainbow trout, Dev. Comp. Immunol. 17 (1993) 419–424, https://doi.org/10.1016/0145-305x(93)90033-m.

[7] G.L. Bullock, D.A. Conroy, S.F. Snieszko, Septicemic diseases caused by motile *Aeromnads* and *Pseudomonads*, in: S.F. Snieszko, H.R. Axelrod (Eds.), Diseases of Fishes, Book 2A: Bacterial Diseases of Fishes, New Jersey, 1971, pp. 21–41, https://doi.org/10.1590/1678-4162-11989.

[8] J.M. Janda, S.L. Abbott, The genus *Aeromonas*: taxonomy, pathogenicity and infection, Clin. Microbiol. Rev. 23 (2010) 35–73, https://doi.org/10.1128/cmr.00039-09.

[9] A. Semwal, A. Kumar, N. Kumar, A review on pathogenicity of *Aeromonas hydrophila* and their mitigation through medicinal herbs in aquaculture, Heliyon 9 (2023), 14088, https://doi.org/10.1016/j.heliyon.2023.e14088.

[10] K.T. Kim, S.H. Lee, K.K. Lee, J.E. Han, D. Kwak, Enhanced virulence of *Aeromonas hydrophila* is induced by stress and serial passaging in mice, Animals (Basel) 11 (2021) 508, https://doi.org/10.3390/ani11020508.

[11] V. Samayanpaulraj, M. Sivaramapillai, S.N. Palani, K. Govindaraj, V. Velu, U. Ramesh, Identification and characterization of virulent *Aeromonas hydrophila* Ah17 from infected *Channa striata* in river Cauvery and in vitro evaluation of shrimp chitosan, Food Sci. Nutr. 8 (2020) 1272–1283, https://doi.org/10.1002/fsn3.1416.

[12] E.J. Nya, B. Austin, Use of garlic, *Allium sativum*, to control *Aeromonas hydrophila* infection in rainbow trout, *Oncorhynchus mykiss* (*Walbaum*), J. Fish. Dis. 32 (2009) 963–970, https://doi.org/10.1111/j.1365-2761.2009.01100.x.

[13] X. Song, X. Hu, B. Sun, Y. Bo, K. Wu, L. Xiao, C. Gong, A transcriptome analysis focusing on inflammation-related genes of grass carp intestines following infection with *Aeromonas hydrophila*, Sci. Rep. 7 (2017), 40777, https://doi.org/10.1038/srep40777.

[14] R. Harikrishnan, M.N. Rani, C. Balasundaram, Hematological and biochemical parameters in common carp, *Cyprinus carpio*, following herbal treatment for *Aeromonas hydrophila* infection, Aquaculture 221 (2003) 41–50, https://doi.org/10.1016/S0044-8486(03)00023-1.

[15] J.W. Pridgeon, P.H. Klesius, Molecular identification and virulence of three *Aeromonas hydrophila* isolates cultured from infected channel catfish during a disease outbreak in west Alabama (USA) in 2009, Dis Aquat Organ 94 (2011) 249–253, https://doi.org/10.3354/dao02332.

[16] D. Xu, P. Han, L. Xia, J. Gan, Q. Xu, A comparative transcriptome analysis focusing on immune responses of Asian swamp eel following infection with *Aeromonas hydrophila*, Aquaculture 539 (2021), 736655, https://doi.org/10.1016/j.aquaculture.2021.736655.

[17] J. Feng, R. Guan, S. Guo, P. Lin, F. Zadlock, Molecular cloning of Japanese eel *Anguilla japonica* TNF-α and characterization of its expression in response to LPS, poly I: C and *Aeromonas hydrophila* infection, Chin J Ocean Limnol 32 (2014) 1046–1059, https://doi.org/10.1007/s00343-014-3231-2.

[18] I. Rodríguez, B. Novoa, A. Figueras, Immune response of zebrafish (*Danio rerio*) against a newly isolated bacterial pathogen *Aeromonas hydrophila*, Fish Shellfish Immunol. 25 (2008) 239–249, https://doi.org/10.1016/j.fsi.2008.05.002.

[19] S. Jinendiran, A.A. Nathan, D. Ramesh, B. Vaseeharan, N. Sivakumar, Modulation of innate immunity, expression of cytokine genes and disease resistance against *Aeromonas hydrophila* infection in goldfish (*Carassius auratus*) by dietary supplementation with *Exiguobacterium acetylicum* S01, Fish Shellfish Immunol. 84 (2019) 458–469, https://doi.org/10.1016/j.fsi.2018.10.026.

[20] M.J.A. Sarkar, M.M. Rashid, Pathogenicity of the bacterial isolate *Aeromonas hydrophila* to catfishes, carps and perch, J. Bangladesh Agric. Univ. 10 (2012) 157–161, https://doi.org/10.22004/ag.econ.209312.

[21] B. Yardimci, Y. Aydin, Pathological findings of experimental *Aeromonas hydrophila* infection in Nile tilapia (*Oreochromis niloticus*), Ankara Univ. Vet. Fak. Derg. 58 (2011) 47–54, https://doi.org/10.1501/Vetfak_0000002448.

[22] V. Samayanpaulraj, V. Velu, R. Uthandakalaipandiyan, Determination of lethal dose of *Aeromonas hydrophila* Ah17 strain in snake head fish *Channa striata*, Microb. Pathog. 127 (2019) 7–11, https://doi.org/10.1016/j.micpath.2018.11.035.

[23] J.W. Jun, J.H. Kim, D. Gomez, C. Jr, J.E. Han, S.P. Shin, S.C. Park, Occurrence of tetracycline-resistant *Aeromonas hydrophila* infection in Korean cyprinid loach (*Misgurnus anguillicaudatus*), Afr. J. Microbiol. Res. 4 (2010) 849–855.

[24] J. Yu, B.H. Koo, D.H. Kim, D.W. Kim, S.W. Park, *Aeromonas sobria* infection in farmed mud loach (*Misgurnus mizolepis*) in Korea, a bacteriological survey, Iran, J Vet Res 16 (2015) 194–201.

[25] Z. Du, D. Wang, N. Zhang, T. Wang, Q. Wu, Z. Xu, Y. Long, L. Jiang, W. Luo, A case of *Aeromonas veronii* infection in golden Taiwanese loach (*Paramisgurnus dabryanus*) at low water temperature, Aquac Res 51 (2019) 1307–1312, https://doi.org/10.1111/are.14459.

[26] R. Roy, M. Bahadur, S. Barat, Isolation, identification and antibiotic resistance of *Aeromonas* spp. and *Salmonella* spp. from the fresh water loach, *Lepidocephalichthys guntea* and water of Terai river Lotchka, West Bengal, India, Zool. Pol. 58 (2013) 5–17, https://doi.org/10.2478/zoop-2013-0001.

[27] R.Y. Chen, B.T. Ngoc Hieu, G. Audira, B. Lou, M.D. Lin, C.D. Hsiao, Meta-transcriptomic analysis of RNAseq data reveals pacu and loach fish with unusually high levels of myoglobin expression in skeletal muscles, Animals (Basel) 10 (2020) 1130, https://doi.org/10.3390/ani10071130.

[28] Z.H. Shang, M. Huang, M.X. Wu, D. Mi, K. You, Y.L. Zhang, Transcriptomic analyses of the acute aerial and ammonia stress response in the gill and liver of large-scale loach (*Paramisgurnus dabryanus*), Comp. Biochem. Physiol. C Toxicol. Pharmacol. 250 (2021), 109185, https://doi.org/10.1016/j.cbpc.2021.109185.

[29] S. Huang, B. Sun, L. Huang, L. Yang, C. Liu, J. Zhu, J. Gao, X. Cao, Comparative transcriptomic analysis of regenerated skins provides insights into cutaneous air-breathing formation in fish, Biology 10 (2021) 1294, https://doi.org/10.3390/biology10121294.

[30] N. Yang, C. Yang, T. Tan, Q. Wang, X. Lei, Histology study and transcriptome analysis of the testis of Loach (*Misgurnus anguillicaudatus*) in response to phenanthrene exposure, Ecotoxicol. Environ. Saf. 242 (2022), 113950, https://doi.org/10.1016/j.ecoenv.2022.113950.

[31] S. Huang, X. Cao, X. Tian, Transcriptomic analysis of compromise between air-breathing and nutrient uptake of posterior intestine in loach (*Misgurnus anguillicaudatus*), an air-breathing fish, Mar. Biotechnol. 18 (2016) 521–533, https://doi.org/10.1007/s10126-016-9713-9.

[32] A.F. Gonçalves, L.F. Castro, C. Pereira-Wilson, J. Coimbra, J.M. Wilson, Is there a compromise between nutrient uptake and gas exchange in the gut of *Misgurnus anguillicaudatus*, an intestinal air-breathing fish? Comp. Biochem. Physiol., Part D: Genomics Proteomics 2 (2007) 345–355, https://doi.org/10.1016/j.cbd.2007.08.002.

[33] J.M. Tomás, The main *Aeromonas* pathogenic factors, ISRN microbiol 2012 (2012) 1–22, https://doi.org/10.5402/2012/256261.

[34] A.L. Gannam, R.M. Schrock, Immunostimulants in fish diets, J Appl Aquac 9 (1999) 53–89, https://doi.org/10.1300/J028v09n04_06.

[35] L. Niklasson, Intestinal Mucosal Immunology of *Salmonids* Response to Stress and Infection and Crosstalk with the Physical Barrier, Gothenburg University, Gothenburg, 2013.

[36] X.D. Ling, W.T. Dong, Y. Zhang, X. Qian, W.D. Zhang, W.H. He, X.X. Zhao, J.X. Liu, Comparative transcriptomics and histopathological analysis of crucian carp infection by atypical A*eromonas salmonicida*, Fish Shellfish Immunol. 94 (2019) 294–307, https://doi.org/10.1016/j.fsi.2019.09.006.

[37] P. Sun, D. Zhang, N. Li, X.F. Li, Y.H. Ma, H. Li, Y. Tian, T. Wang, S.A. Siddiquid, W.W. Sun, L. Zhang, Transcriptomic insights into the immune response of the intestine to *Aeromonas veronii* infection in northern snakehead (*Channa argus*), Ecotoxicol. Environ. Saf. 255 (2023), 114825, https://doi.org/10.1016/j.ecoenv.2023.114825.

[38] C. Pan, Y. Zhu, K. Cao, J. Li, S. Wang, J. Zhu, X. Zeng, H. Zhang, Z. Qin, Transcriptome, intestinal microbiome and histomorphology profiling of differences in the response of Chinese sea bass (*Lateolabrax maculatus*) to *Aeromonas hydrophila* infection, Front. Microbiol. 24 (2023), 1103412, https://doi.org/10.3389/fmicb.2023.1103412.

[39] G.C. Davey, J.A. Calduch-Giner, B. Houeix, A. Talbot, A. Sitjà-Bobadilla, P. Prunet, J. Pérez-Sánchez, M.T. Cairns, Molecular profiling of the gilthead sea bream (*Sparus aurata L.*) response to chronic exposure to the myxosporean parasite *Enteromyxum leei*, Mol. Immunol. 48 (2011) 2102–2112, https://doi.org/10.1016/j.molimm.2011.07.003.

[40] X. Zhang, L. Ding, Y. Yu, W. Kong, Y. Yin, Z. Huang, X. Zhang, Z. Xu, The change of teleost skin commensal microbiota is associated with skin mucosal transcriptomic responses during parasitic infection by *Ichthyophthirius multifillis*, Front. Immunol. 9 (2018) 2972, https://doi.org/10.3389/fimmu.2018.02972.

[41] P. Elumalai, A.S. Rubeena, J. Arockiaraj, R. Wongpanya, M. Cammarata, E. Ringø, B. Vaseeharan, The role of lectins in finfish: a review, Rev Fish Sci Aquac 27 (2019) 152–169, https://doi.org/10.1080/23308249.2018.1520191.

[42] J. Vandooren, Y. Itoh, Alpha-2-Macroglobulin in inflammation, immunity and infections, Front. Immunol. 12 (2021), 803244, https://doi.org/10.3389/fimmu.2021.803244.

[43] C. Sun, S. Zhang, Immune-Relevant and antioxidant activities of vitellogenin and yolk proteins in fish, Nutrients. 7 (2015) 8818–8829.

[44] C. Yang, M. Jiang, F. Wu, L. Yu, J. Tian, W. Liu, X. Lu, H. Wen, Identification of a C-type lectin from tilapia (*Oreochromis niloticus*) and its functional characterization under low-temperature stress, Fish Shellfish Immunol. 58 (2016) 631–640, https://doi.org/10.1016/j.fsi.2016.10.004.

[45] S.A. Ragland, A.K. Criss, From bacterial killing to immune modulation: recent insights into the functions of lysozyme, PLoS Pathog. 13 (2017), 1006512, https://doi.org/10.1371/journal.ppat.1006512.

[46] X. Romero, J. Sintes, P. Engel, Role of SLAM family receptors and specific adapter SAP in innate-like lymphocytes, Crit. Rev. Immunol. 34 (2014) 263–299, https://doi.org/10.1615/critrevimmunol.2014010538.

[47] K. Murakami, M. Tanaka, T. Usui, D. Kawabata, A. Shiomi, M.I. Hashimoto, M. Shimizu, N. Yukawa, H. Yoshifuji, T. Nojima, K. Ohmura, T. Fujii, H. Umehara, T. Mimori, Follistatin-related protein/follistatin-like 1 evokes an innate immune response via CD14 and toll-like receptor 4, FEBS Lett. 586 (2012) 319–324, https://doi.org/10.1016/j.febslet.2012.01.010.

[48] M.X. Chang, F. Xiong, X.M. Wu, Y.W. Hu, The expanding and function of NLRC3 or NLRC3-like in teleost fish: recent advances and novel insights, Dev. Comp. Immunol. 114 (2021), 103859, https://doi.org/10.1016/j.dci.2020.103859.

[49] H. Chen, S. Ding, J. Tan, D. Yang, Y. Zhang, Q. Liu, Characterization of the Japanese flounder NLRP3 inflammasome in restricting *Edwardsiella piscicida* colonization in vivo, Fish Shellfish Immunol. 103 (2020) 169–180, https://doi.org/10.1016/j.fsi.2020.04.063.

[50] W. Huang, S. Ghisletti, K. Saijo, M. Gandhi, M. Aouadi, G.J. Tesz, D.X. Zhang, J. Yao, M.P. Czech, B.L. Goode, M.G. Rosenfeld, C.K. Glass, Coronin 2A mediates actin-dependent de-repression of inflammatory response genes, Nature 470 (2011) 414–418, https://doi.org/10.1038/nature09703.

[51] J. Wang, Z. Jia, H. Dang, J. Zou, Meteorin-like/Meteorin-β upregulates proinflammatory cytokines via NF-κB pathway in grass carp *Ctenopharyngodon idella*, Dev. Comp. Immunol. 127 (2022), 104289, https://doi.org/10.1016/j.dci.2021.104289.

[52] V. Kumaresan, M. Pasupuleti, B.A. Paray, M.K. Al-Sadoon, J. Arockiaraj, Gene profiling of antimicrobial peptides, complement factors and MHC molecules from the skin transcriptome of *Channa striatus* and its expression pattern during *Aeromonas hydrophila* infection, Fish Shellfish Immunol. 84 (2019) 48–55, https://doi.org/10.1016/j.fsi.2018.09.061.

[53] D.M.K.P. Sirisena, M.D.N. Tharuka, D.S. Liyanage, S. Jung, M.J. Kim, J. Lee, An interferon-induced GTP-binding protein, Mx, from the redlip mullet, *Liza haematocheila*: deciphering its structural features and immune function, Fish Shellfish Immunol. 96 (2020) 279–289, https://doi.org/10.1016/j.fsi.2019.11.063.

[54] C.A. Jefferies, Regulating IRFs in IFN driven disease, Front. Immunol. 10 (2019) 325, https://doi.org/10.3389/fimmu.2019.00325.

[55] F. Biet, C. Locht, L. Kremer, Immunoregulatory functions of interleukin 18 and its role in defense against bacterial pathogens, J. Mol. Med. (Berl.) 80 (2002) 147–162, https://doi.org/10.1007/s00109-001-0307-1.

[56] W. Zhu, J. Su, Immune functions of phagocytic blood cells in teleost, Rev Aquac 14 (2022) 630–646, https://doi.org/10.1111/raq.12616.

[57] J. Kaufman, J. Salomonsen, M. Flajnik, Evolutionary conservation of MHC class I and class II molecules-different yet the same, in: Seminars in Immunology, Academic Press, 1994, pp. 411–424, https://doi.org/10.1006/smim.1994.1050.

[58] H.R. Kim, J.S. Park, H. Karabulut, F. Yasmin, C.D. Jun, Transgelin-2: a double-edged sword in immunity and cancer metastasis, Front. Cell Dev. Biol. 9 (2021), 606149, https://doi.org/10.3389/fcell.2021.606149.

[59] M.L. Rise, S.R. Jones, G.D. Brown, K.R. von Schalburg, W.S. Davidson, B.F. Koop, Microarray analyses identify molecular biomarkers of Atlantic salmon macrophage and hematopoietic kidney response to *Piscirickettsia salmonis* infection, Physiol genomics 20 (2004) 21–35, https://doi.org/10.1152/physiolgenomics.00036.2004.

[60] M. Rozas-Serri, A. Pena, L. Maldonado, Transcriptomic profiles of post-smolt Atlantic salmon challenged with *Piscirickettsia salmonis* reveal a strategy to evade the adaptive immune response and modify cell-autonomous immunity, Dev. Comp. Immunol. 81 (2018) 348–362, https://doi.org/10.1016/j.dci.2017.12.023.

[61] S. Mostowy, A.R. Shenoy, The cytoskeleton in cell-autonomous immunity: structural determinants of host defence, Nat. Rev. Immunol. 15 (2015) 559–573, https://doi.org/10.1038/nri3877.

[62] R.J. Robb, G.R. Hill, The interferon-dependent orchestration of innate and adaptive immunity after transplantation, Blood 119 (2012) 5351–5358, https://doi.org/10.1182/blood-2012-02-368076.

[63] F. Velotti, I. Barchetta, F.A. Cimini, M.G. Cavallo, Granzyme B in inflammatory diseases: apoptosis, inflammation, extracellular matrix remodeling, epithelial-to-mesenchymal transition and fibrosis, Front. Immunol. 11 (2020), 587581, https://doi.org/10.3389/fimmu.2020.587581.

[64] Z. Wang, C. Xie, Y. Li, J. Cai, J. Tang, J. Jian, K.W.H. Kwok, Y. Lu, Molecular characterization and expression of CD48 in Nile tilapia (*Oreochromis niloticus*) in response to different stimulus, Fish Shellfish Immunol. 97 (2020) 515–522, https://doi.org/10.1016/j.fsi.2019.12.034.

[65] S.C. Fagerholm, H.S. Lek, V.L. Morrison, Kindlin-3 in the immune system, Am J Clin Exp Immunol 3 (2014) 37–42.

[66] J.R. Hwang, Y. Byeon, D. Kim, S.G. Park, Recent insights of T cell receptor-mediated signaling pathways for T cell activation and development, Exp. Mol. Med. 52 (2020) 750–761, https://doi.org/10.1038/s12276-020-0435-8.

[67] J. Li, W. Liang, K. Li, X. Jiao, K. Ai, Y. Zhang, X. Wei, J. Yang, ZAP70 activation is an early event of T cell immunity that involved in the anti-bacterial adaptive immune response of Nile tilapia, Dev. Comp. Immunol. 124 (2021) 104–177, https://doi.org/10.1016/j.dci.2021.104177.

[68] H.J. Wang, L.X. Xiang, J.Z. Shao, S. Jia, Molecular cloning, characterization and expression analysis of an IL-21 homologue from *Tetraodon nigroviridis*, Cytokine 35 (2006) 126–134, https://doi.org/10.1016/j.cyto.2006.07.010.

[69] I. Horváth, G. Multhoff, A. Sonnleitner, L. Vígh, Membrane-associated stress proteins: more than simply chaperones, Biochimica Biophys Acta 1778 (2008) 1653–1664, https://doi.org/10.1016/j.bbamem.2008.02.012.

[70] H.Y. Tan, S.W. Chen, S.Y. Hu, Improvements in the growth performance, immunity, disease resistance, and gut microbiota by the probiotic *Rummeliibacillus stabekisii* in Nile tilapia (*Oreochromis niloticus*), Fish Shellfish Immunol. 92 (2019) 265–275, https://doi.org/10.1016/j.fsi.2019.06.027.

[71] Z. Liu, S.W. Wu, C.Q. Lei, Q. Zhou, S. Li, H.B. Shu, Y.Y. Wang, Heat shock cognate 71 (HSC71) regulates cellular antiviral response by impairing formation of VISA aggregates, Protein Cell 4 (2013) 373–382, https://doi.org/10.1007/s13238-013-3902-3.

[72] Y. Xie, L. Song, Z. Weng, S. Liu, Z. Liu, Hsp90, Hsp60 and sHsp families of heat shock protein genes in channel catfish and their expression after bacterial infections, Fish Shellfish Immunol. 44 (2015) 642–651, https://doi.org/10.1016/j.fsi.2015.03.027.

[73] W. Zhou, Y. Zhang, Y. Wen, W. Ji, Y. Zhou, Y. Ji, X. Liu, W. Wang, M. Asim, X. Liang, T. Ai, Analysis of the transcriptomic profilings of Mandarin fish (*Siniperca chuatsi*) infected with *Flavobacterium columnare* with an emphasis on immune responses, Fish Shellfish Immunol. 43 (2015) 111–119, https://doi.org/10.1016/j.fsi.2014.12.006.

[74] W. Rungrassamee, R. Leelatanawit, P. Jiravanichpaisal, S. Klinbunga, N. Karoonuthaisiri, Expression and distribution of three heat shock protein genes under heat shock stress and under exposure to *Vibrio harveyi* in *Penaeus monodon*, Dev. Comp. Immunol. 34 (2010) 1082–1089, https://doi.org/10.1016/j.dci.2010.05.012.

[75] K. Syahputra, P.W. Kania, A. Al-Jubury, H. Marnis, H. Mathiessen, R.P. Dirks, K. Buchmann, Association between stress, metabolism, and growth in *Ichthyophthirius multifiliis* infected rainbow trout gills: transcriptomic evidence, Aquaculture 526 (2020), 735384, https://doi.org/10.1016/j.aquaculture.2020.735384.
[76] Y. Xu, Y. Yu, X. Zhang, Z. Huang, H. Li, S. Dong, Y. Liu, F. Dong, Z. Xu, Molecular characterization and expression analysis of complement component 3 in dojo loach (*Misgurnus anguillicaudatus*), Fish Shellfish Immunol. 72 (2018) 484–493, https://doi.org/10.1016/j.fsi.2017.11.022.
[77] A.M. Bolger, M. Lohse, B. Usadel, Trimmomatic: a flexible trimmer for Illumina sequence data, Bioinformatics 30 (2014) 2114–2120, https://doi.org/10.1093/bioinformatics/btu170.
[78] R. Henschel, M. Lieber, L. Wu, P.M. Nista, B.J. Haas, R.D. LeDuc, Trinity RNA-seq assembler performance optimization, Proceedings of the 1st Conference of the Extreme Science and Engineering Discovery Environment: Bridging from the extreme to the campus and beyond 45 (2012) 1–8, https://doi.org/10.1145/2335755.2335842.
[79] W. Li, A. Godzik, Cd-hit, A fast program for clustering and comparing large sets of protein or nucleotide sequences, Bioinformatics 22 (2006) 1658–1659, https://doi.org/10.1093/bioinformatics/btl158.
[80] B. Buchfink, C. Xie, D. Huson, Fast and sensitive protein alignment using DIAMOND, Nat. Methods 12 (2015) 59–60, https://doi.org/10.1038/nmeth.3176.
[81] A. Conesa, S. Götz, J.M. García-Gómez, J. Terol, M. Talón, M. Robles, Blast2GO: a universal tool for annotation, visualization and analysis in functional genomics research, Bioinformatics 21 (2005) 3674–3676, https://doi.org/10.1093/bioinformatics/bti610.
[82] Y. Moriya, M. Itoh, S. Okuda, A.C. Yoshizawa, M. Kanehisa, KAAS: an automatic genome annotation and pathway reconstruction server, Nucleic Acids Res. 35 (2007) 182–185, https://doi.org/10.1093/nar/gkm321.
[83] S. Anders, W. Huber, Differential Expression of RNA-Seq Data at the Gene Level - the DESeq Package, EMBL, Heidelberg, Germany, 2012.
[84] H. Liu, M.S. Lamm, K. Rutherford, M.A. Black, J.R. Godwin, N.J. Gemmell, Large-scale transcriptome sequencing reveals novel expression patterns for key sex-related genes in a sex-changing fish, Biol. Sex Differ. 6 (2015) 26, https://doi.org/10.1186/s13293-015-0044-8.
[85] A. Saco, M. R Campos, B. Novoa, A. Figueras, Mussel antiviral transcriptome response and elimination of viral haemorrhagic septicaemia virus (VHSV), Fish Shellfish Immunol. 136 (2023), 108735, https://doi.org/10.1016/j.fsi.2023.108735.
[86] D. Szklarczyk, A.L. Gable, K.C. Nastou, D. Lyon, R. Kirsch, S. Pyysalo, N.T. Doncheva, M. Legeay, T. Fang, P. Bork, L.J. Jensen, C. Mering, The STRING database in 2021: customizable protein-protein networks, and functional characterization of user-uploaded gene/measurement sets, Nucleic Acids Res. 49 (2021) 605–612, https://doi.org/10.1093/nar/gkaa1074.
[87] L.J. Jensen, M. Kuhn, M. Stark, S. Chaffron, C. Creevey, J. Muller, T. Doerks, P. Julien, A. Roth, M. Simonovic, P. Bork, C. Mering, STRING 8–a global view on proteins and their functional interactions in 630 organisms, Nucleic Acids Res. 37 (2009) 412–416, https://doi.org/10.1093/nar/gkn760.